Extravascular Transport of Drugs in Tumor Tissue: Effect of Lipophilicity on Diffusion of Tirapazamine Analogues in Multicellular Layer Cultures

Frederik B. Pruijn,* Joanna R. Sturman, H. D. Sarath Liyanage, Kevin O. Hicks, Michael P. Hay, and William R. Wilson

Auckland Cancer Society Research Centre, Faculty of Medical and Health Sciences, The University of Auckland, Private Bag 92019, Auckland, New Zealand

Received June 8, 2004

The extravascular diffusion of antitumor agents is a key determinant of their therapeutic activity, but the relationships between physicochemical properties of drugs and their extravascular transport are poorly understood. It is well-known that drug lipophilicity plays an important role in transport across biological membranes, but the net effect of lipophilicity on transport through multiple layers of tumor cells is less clear. This study examines the influence of lipophilicity (measured as the octanol−water partition coefficient P) on the extravascular transport properties of the hypoxic cytotoxin tirapazamine (TPZ, **1**) and a series of 13 neutral analogues, using multicellular layers (MCLs) of HT29 human colon carcinoma cells as an in vitro model for the extravascular compartment of tumors. Flux of drugs across MCLs was determined using diffusion chambers, with the concentration−time profile on both sides of the MCL measured by HPLC. Diffusion coefficients in the MCLs (D_{MCL}) were inversely proportional to $M_r^{0.5}$ (M_r, relative molecular weight), although this was a minor contributor to differences between compounds over the narrow M_r range investigated. Differences in lipophilicity had a larger effect, with a sigmoidal dependence of D_{MCL} on log P. Correcting for M_r differences, lipophilic compounds (log $P > 1.5$) had ca. 15-fold higher D_{MCL} than hydrophilic compounds (log $P < -1$). Using a pharmacokinetic/pharmacodynamic (PK/PD) model in which diffusion in the extravascular compartment of tumors is considered explicitly, we demonstrated that hypoxic cell kill is very sensitive to changes in extravascular diffusion coefficient of TPZ analogues within this range. This study shows that simple monosubstitution of TPZ can alter log P enough to markedly improve extravascular transport and activity against target cells, especially if rates of metabolic activation are also optimized.

Introduction

To reach their target cells in solid tumors, most antitumor agents must diffuse through the extravascular compartment. The importance of this problem is well-recognized for high M_r (relative molecular weight) therapeutic agents such as antibodies and other complex biological molecules;[1,2] less is understood about extravascular transport of small molecule drugs, although it has been suspected for decades that this is a significant limitation in the chemotherapy of solid tumors.[3−9] This problem is expected to be particularly important for hypoxic cytotoxins such as tirapazamine (TPZ; 1,2,4-benzotriazin-3-amine 1,4-dioxide, **1**)[10,11] since these must diffuse relatively large distances from functional blood vessels to reach their target (hypoxic) cells. In addition, TPZ, like most other hypoxic cytotoxins, is activated by metabolism under hypoxia[12,13] and will necessarily be consumed as it diffuses into hypoxic zones. Studies with hypoxic 3D cell cultures have confirmed that TPZ is metabolized rapidly enough to impede its penetration into hypoxic zones.[14−18] It may be feasible to improve the diffusion range of TPZ by designing analogues with higher diffusion coefficients in tissue, but the required theoretical framework (i.e., knowledge of the relationship between drug physicochemical properties and transport parameters) is lacking.

The available evidence suggests that TPZ, like many other anticancer drugs, enters cells by passive diffusion.[13,18] Given the well-established relationship between lipophilicity (typically measured by the octanol−water partition coefficient P) and plasma membrane permeability for small molecules,[19,20] it is a reasonable hypothesis that lipophilic drugs will be able to access the transcellular transport route (through cells), while more hydrophilic drugs will be confined to the paracellular route (between cells). Depending on the interstitial volume fraction, tortuosity of the extracellular path, and matrix composition, restriction to the paracellular route has the potential to greatly slow transport. Therefore, it is reasonable to expect P to be a determinant of extravascular transport in tumors. However, to our knowledge, there has not been any direct or quantitative determination of the effect of lipophilicity on the ability of anticancer drugs (or other molecules) to diffuse the large intercapillary distances typical of tumors.

We and others have developed a novel experimental model for measuring the extravascular diffusion coefficients of anticancer drugs (Figure 1).[15,21,22] In this model, tumor cells are grown on permeable collagen-coated Teflon support membranes to form a multicellular layer (MCL) of up to 20 cell layers in thickness at

* To whom corespondence should be addressed. Phone: 64-9-3737599, extension 86939. Fax: 64-9-3737571. E-mail: f.pruijn@auckland.ac.nz.

10.1021/jm049549p CCC: $30.25
Published on Web 01/27/2005

Scheme 1[a]

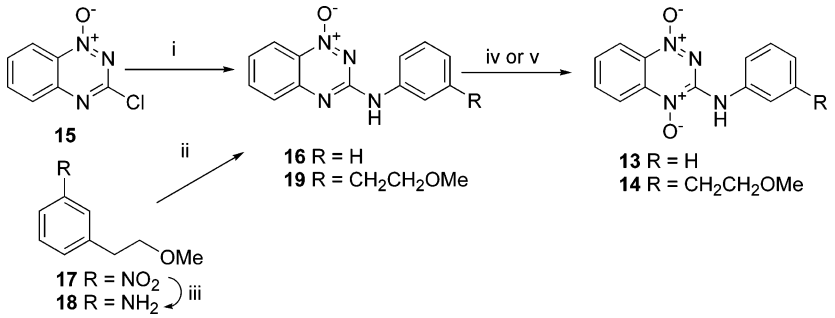

[a] Reagents: (i) concentrated HCl, aniline, DME; (ii) **15** + **18**, DMSO; (iii) H_2, Pd/C, EtOH; (iv) MCPBA, DCM; (v) CF_3CO_3H, $CHCl_3$.

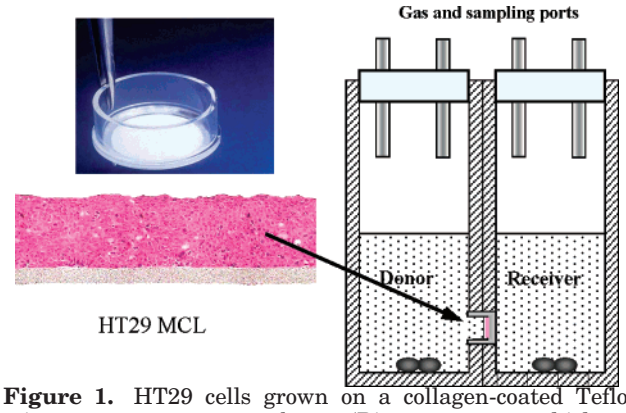

Figure 1. HT29 cells grown on a collagen-coated Teflon microporous support membrane (Biopore, average thickness 30 μm) in Millicell-CM cell culture inserts (Millipore) (H & E stained frozen section). Drug diffusion is measured in a diffusion chamber that separates two compartments (donor and receiver) that each hold about 5.5 mL of well-stirred culture medium at 37 °C.

tissue-like cell densities. These 3D structures eventually become diffusion-limited, with central hypoxia and necrosis,[15,21] and thus mimic the extravascular compartment in tumors. The simple planar geometry of MCLs allows direct measurement of drug transport by quantifying the flux of drug across an MCL that separates two well-stirred compartments in a diffusion chamber.[23] The concentrations of the drug and its metabolites, in the "donor" and "receiver" compartments, can be fitted to Fick's second law (with added reaction terms for reversible binding and/or metabolism when appropriate) to provide the apparent diffusion coefficient in the MCL (D_{MCL}). This parameter can then be used, in conjunction with the plasma pharmacokinetics (PK), to develop a distributed parameter (i.e., spatially resolved) PK model that describes the concentration−time profile of the drug at each position within the extravascular compartment. This PK model is coupled to a pharmacodynamic (PD) model that describes the biological response (e.g., tumor cell kill) as a function of concentration and time, allowing prediction of activity against cells as a function of distance from blood vessels.[18,23]

In this study, we examine the influence of lipophilicity on the diffusion of a series of neutral analogues of TPZ in MCL cultures grown from the human colon carcinoma cell line HT29. To minimize the effects of bioreductive drug metabolism, the experiments were conducted using high ambient oxygen concentrations (95% in the gas phase), which reoxygenates the central hypoxic zone in MCLs.[15] We use this approach to define the relationship between log P and D_{MCL}. In addition, we use a distributed parameter PK/PD model to examine the effect of changing the D_{MCL} of TPZ on hypoxic cell killing in tumor tissue.

Chemistry

TPZ (**1**) and the analogues **2**−**12** were synthesized in this laboratory as previously reported.[24] Reaction of chloride[25] **15** with aniline gave 1-oxide **16**[26] which was oxidized with MCPBA to give 1,4-dioxide **13** (Scheme 1). Similarly, reaction of chloride **15** with aniline **18**, prepared from nitrobenzene **17**,[27] gave the 1-oxide **19** that was oxidized with trifluoroperacetic acid to the 1,4-dioxide **14**.

Methods

Partition Coefficients. The octanol−water partition coefficients (P) of TPZ (**1**) and **2**−**14** were measured using the shake-flask method,[28] with analysis by HPLC.

MCL Cultures. MCLs were grown from human HT29 colon carcinoma cells as described elsewhere.[18,29] In brief, 1×10^6 cells were seeded on collagen-coated Teflon microporous support membranes in Millicell-CM cell culture inserts and grown for 3 days submerged in stirred culture medium supplemented with 10% fetal calf serum.

Determination of Diffusion Coefficient in MCLs. Flux through MCLs was measured in a diffusion chamber as described.[23] TPZ analogues were added to the "donor" compartment to 50 μM, along with the flux markers [^{14}C]urea, D-[2-^{3}H]mannitol, and 9(10*H*)-acridone. The diffusion of each compound was also determined in the collagen-coated Teflon porous support membrane without an MCL present. Samples were taken from both the donor and receiver compartment for up to 5 h. An aliquot was assayed for radioactivity by dual-label liquid scintillation counting, and the balance was analyzed by HPLC. The concentration−time profiles were numerically fitted to Fick's second law to derive D_{MCL} with addition of reaction terms in the MCL when necessary, and the effective diffusion coefficient in the support membrane (D_s).[23,23] The latter parameter reflects diffusion through the aqueous pores in the support membrane but also takes into account the unstirred boundary layers on each side of the membrane.

Results and Discussion

The relationship between octanol−water partition coefficient P and the diffusion coefficient in MCLs (D_{MCL}) was investigated for TPZ and the 13 analogues shown

Table 1. Structures of Compounds, Octanol−Water Partition Coefficients (P), and Diffusion Coefficients in Teflon Support Membranes (D_s) and HT29 MCLs[a] (D_{MCL})

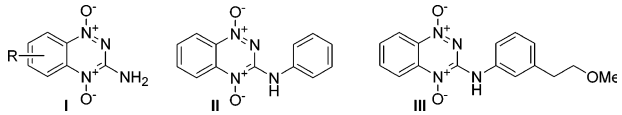

compd	formula	R	M_r (Da)	log P[b]	D_s ($\times 10^{-6}$ cm^2 s^{-1})[b]	D_{MCL} ($\times 10^{-6}$ cm^2 s^{-1})[b]
acridone			195	2.975 ± 0.006 (52)	1.12 ± 0.02 (34)	3.17 ± 0.05 (60)
mannitol			182	−2.616 ± 0.002 (6)	1.22 ± 0.03 (6)	0.21 ± 0.01 (32)
urea			60	−2.01 ± 0.01 (6)	2.08 ± 0.05 (19)[c]	0.45 ± 0.02 (6)[c]
1 (TPZ)	I		178	−0.342 ± 0.005 (6)	1.26 ± 0.04 (5)[c]	0.40 ± 0.01 (12)[c]
2	I	6-Me	192	0.068 ± 0.007 (3)	1.38	0.54 ± 0.03 (3)
3	I	7-Me	192	0.127 ± 0.001 (3)	1.2 ± 0.1 (2)	0.66 ± 0.02 (2)
4	I	8-Me	192	0.24 ± 0.01 (3)	1.32 ± 0.06 (2)	0.75 ± 0.02 (2)
5	I	7-SO_2Me	256	−1.15 ± 0.02 (3)	1.22 ± 0.08 (2)	0.21 ± 0.03 (2)
6	I	8-SO_2Me	256	−1.382 ± 0.006 (3)	1.15 ± 0.02 (2)	0.32 ± 0.03 (2)
7	I	5-Cl	212	−0.102 ± 0.008 (3)	1.05 ± 0.09 (2)	0.35 ± 0.01 (2)
8	I	7-Cl	212	0.441 ± 0.003 (3)	1.22 ± 0.08 (2)	0.87 ± 0.02 (2)
9	I	8-Cl	212	0.166 ± 0.002 (3)	1.3 ± 0.1 (2)	0.67 ± 0.04 (2)
10	I	7-CF_3	246	0.82 ± 0.01 (3)	1.19 ± 0.01 (2)	0.90 ± 0.06 (2)
11	I	8-CF_3	246	0.48 ± 0.01 (3)	1.30 ± 0.09 (2)	0.52 ± 0.01 (2)
12	I	8-NEt_2	249	0.830 ± 0.003 (3)	0.86 ± 0.02 (2)	0.45 ± 0.02 (2)
13	II		254	1.425 ± 0.005 (6)	1.01 ± 0.09 (2)	2.70 ± 0.06 (2)
14	III		312	1.508 ± 0.007 (3)	0.83 ± 0.02 (2)	2.40 ± 0.01 (2)

[a] MCL = multicellular layer. [b] Mean ± SEM or range with number of measurements in parentheses. [c] From Hicks et al.[18]

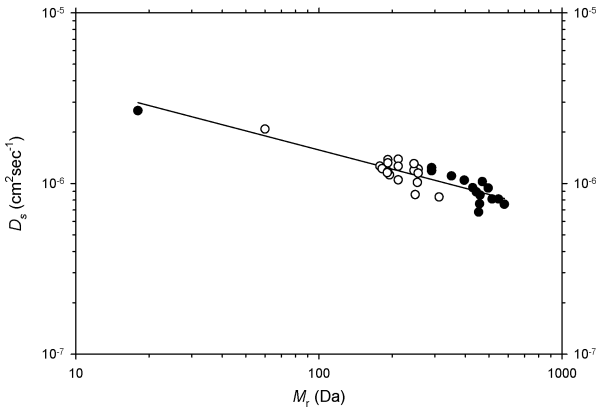

Figure 2. M_r dependence of diffusion coefficients (D_s) in collagen-coated Teflon membranes used to support MCL growth. Flux was measured in αMEM culture medium supplemented with 10% fetal calf serum at 37 °C. The compounds (including the flux markers) of Table 1 are denoted by the open symbols. The line is a linear regression, with slope −0.37.

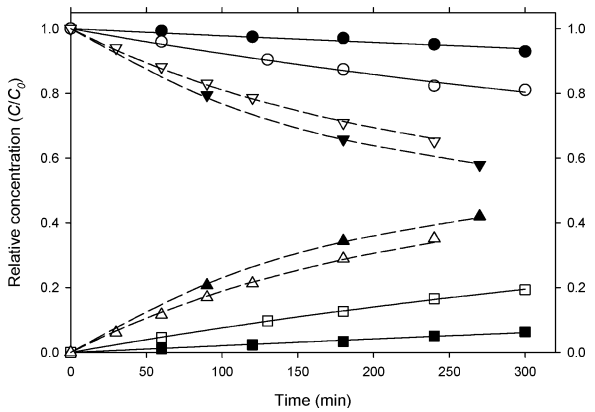

Figure 3. Concentrations of TPZ (**1**, closed symbols) and compound **14** (open symbols) as a function of time in the donor (circles and down triangles) and receiver (squares and up triangles) compartments during a representative flux experiment with HT29 MCLs (solid lines) or Teflon support membranes (dashed lines) under 95% O_2 at 37 °C. Concentrations (C) were normalized against the initial concentration in the donor compartment (C_0; 50 μM). The lines are fits to a simple Fickian diffusion model, based on the average thickness of each MCL as estimated from the flux of the internal standard urea (not shown). Flux of **14** was faster than for TPZ, despite a slightly greater thickness of the MCL used for **14** (167 μm) than for TPZ (149 μm).

in Table 1, along with three internal standards that were included in all experiments. The standards were mannitol (a marker of the paracellular transport route), 9(10*H*)-acridone (a marker of the transcellular route), and urea (used to determine thickness of each MCL). The measured values of P for these 17 compounds spanned almost 6 orders of magnitude.

To interpret the MCL flux data, we first determined the effective diffusion coefficient of each compound through the collagen-coated Teflon support membranes (D_s) on which the MCLs are grown (Figure 2). These membranes have previously been shown to have an effective porosity of ca. 11%;[23] this estimate includes the effect of unstirred boundary layers. Given their large pore size (0.4 μm), D_s is therefore expected to be approximately 11% of the diffusion coefficient in culture medium for all compounds. In each case, the flux curves (concentration−time profiles in the two compartments of the diffusion chamber as illustrated for TPZ and compound **14** in Figure 3) were well-fitted by a simple Fickian diffusion model, with no significant loss of total drug over at least 5 h, confirming chemical stability and lack of binding to any components of the apparatus. Fitted values of D_s showed little variation between compounds (Table 1), as expected, given the narrow range of M_r. Taking a broader set of compounds (including ^3H_2O, the internal standards, and 16 other compounds chemically unrelated to TPZ such as quaternary ammonium salts, dinitrobenzamides, and DNA intercalators), a significant relationship could be demonstrated between D_s and M_r (Figure 2). The regression line in Figure 2 ($N = 34$, $R^2 = 0.81$, $F = 136$) has a slope of −0.37, indicating that D_s is inversely proportional to $M_r^{0.37}$. This is not significantly different from the

theoretical dependence ($M_r^{0.33}$) for spherical molecules in water according to the Stokes−Einstein equation.[30]

In contrast to the narrow range of D_s values for the TPZ analogues, diffusion through MCLs differed considerably between compounds. This is illustrated for TPZ and a lipophilic analogue (**13**) in Figure 3; although the latter compound diffused slightly more slowly than TPZ through bare support membranes (Figure 2), it diffused much more rapidly through MCLs. For both compounds, mass balance was preserved (the total amount of compound in both compartments did not change with time), no metabolites were detected in the chromatograms, and the flux curves were well fitted as simple diffusion. Thus, metabolism in the MCLs was not a factor for these compounds at the high O_2 concentrations used in this study. It is important to note that TPZ is not a known substrate for drug transporters such as P-gp or MRP1 or -2 and that HT29 cells do not express significant levels of these proteins;[31] thus simple passive diffusion is the expected transport mode.

This same approach was used to investigate the other TPZ analogues. Most were also metabolically stable in HT29 MCLs, but six of the compounds with electron-withdrawing substituents (7- and 8-SO_2Me, 5- and 8-Cl, 7- and 8-CF_3) were metabolized significantly (negative mass balance and metabolite peaks in the chromatograms; in some cases these metabolites were identified as the corresponding 1-oxides resulting from two-electron reduction of the 4-oxide moiety by DT-diaphorase; F. B. Pruijn and A. V. Patterson, unpublished data). For these compounds, diffusion coefficients could be estimated by fitting a first-order metabolism term and D_{MCL} simultaneously. The rate constants for metabolism within the MCLs were 0.24 min^{-1} for **5**, 0.44 min^{-1} for **6**, 0.07 min^{-1} for **7**, 3.41 min^{-1} for **9**, 0.35 min^{-1} for **10**, and 1.84 min^{-1} for **11**.

The values of D_{MCL} obtained by modeling the fluxes as diffusion (with metabolism when appropriate) are shown in Table 1. Regression analysis demonstrated a statistically significant relationship between D_{MCL} and log P for all the compounds of Table 1, using a semiempirical three-parameter sigmoidal function (eq 1; R = 0.933, F = 20.25, SE = 0.143),

$$\log(D_{MCL}) = C - [a \log(M_r)] + f(\log P) \qquad (1)$$

where

$$f(\log P) = \frac{\alpha}{1 + e^{-(\log P - \beta)/\gamma}}$$

and where C is a constant and a, α, β, and γ are regression coefficients. The fitted values were $C = -5.6$, $a = 0.5$, $\alpha = 1.2$, $\beta = 0.7$, and $\gamma = 0.6$. Inclusion of the M_r term reduced the variance slightly (with the R value increasing from 0.917 when $a = 0$), but the F-statistic for addition of this term was only 2.80, and this was not statistically significant (P = 0.12). Although the overall statistics of eq 1 did not improve significantly on adding the M_r term (with this set of compounds falling within a relatively narrow size range), there are strong a priori reasons to include this term since on theoretical grounds one would expect a size-dependence at least as marked as for D_s (vide supra). Consistent with expectation, the M_r dependence ($M_r^{-0.5}$) was similar to that observed in aqueous media ($M_r^{-0.37}$) and in good agreement with the observed molecular weight dependence of the permeability surface area product of animal muscle capillary wall ($M_r^{-0.51}$) and of human muscle ($M_r^{-0.50}$).[32]

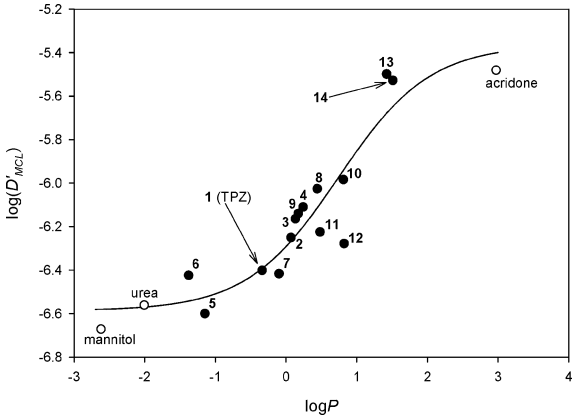

Figure 4. The log P dependence of diffusion coefficients in HT29 MCLs, corrected for differences in molecular size (D'_{MCL}, corrected to the same M_r as TPZ (**1**)) for flux markers (open symbols) and TPZ analogues (closed symbols). Error bars (see Table 1) have been omitted for clarity; numbers refer to TPZ analogues as in Table 1. The line is the fit to a modified form of eq 1 in which the M_r dependence is removed by normalizing to the M_r of TPZ (R = 0.941, F = 33.47, SE = 0.138).

To clarify the log P dependence of D_{MCL}, we normalized for differences in size of the molecules by calculating the expected diffusion coefficient at the same M_r as TPZ (D'_{MCL}), using the M_r dependence determined in eq 1. These size-corrected values, plotted in Figure 4, showed an increase from approximately 0.3×10^{-6} cm^2 s^{-1} for hydrophilic molecules to a 15-fold higher value for the most lipophilic examples. The latter is approximately 3-fold lower than D' in water (calculated using D of urea in water[30] as 8.76×10^{-6} cm^2 s^{-1} at an M_r of 178 Da). The dependence on log P is interpreted as reflecting a transition from paracellular to transcellular transport, with the more hydrophilic analogues effectively restricted to the extracellular diffusion path. These findings are similar to those reported for passive diffusion in epithelial monolayers (e.g., Caco-2). For example, a sigmoidal curve was obtained for the logarithm of the apparent permeability coefficient of β-blockers against the logarithm of the distribution coefficient (i.e., lipophilicity) in Caco-2 monolayers,[33,34] which was interpreted in terms of the relative contributions of trans- and paracellular diffusion barriers.[34] Such an experimental relationship can also be derived from theoretical considerations.[35] The highest achievable D_{MCL} (i.e., the asymptote of the sigmoidal function) is presumably determined mainly by the microviscosity of cytosol but also to some extent of lipoidal membranes and extracellular matrix and is within the range of 2- to 5-fold lower diffusion coefficient for small molecules in cytoplasm in a variety of cell systems.[36]

The log P dependence in the present study indicates that a large (10-fold) increase in the effective diffusion coefficient relative to TPZ in tissue can be achieved by designing compounds with sufficient lipophilicity to permeate plasma membranes efficiently. We next asked whether the observed changes in D_{MCL} are large enough to have a major effect on the ability of TPZ analogues

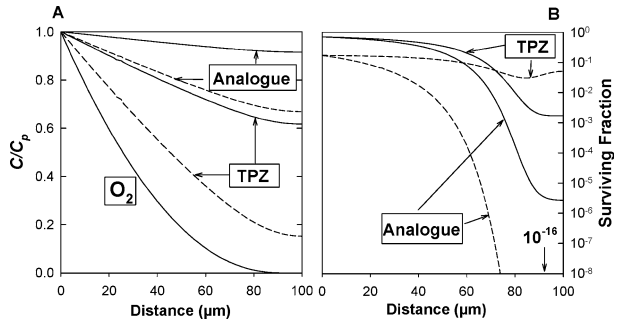

Figure 5. Sensitivity of hypoxic cell killing in tumors to changes in diffusion coefficient of TPZ analogues, simulated using a spatially resolved PK/PD model as described in the Experimental Section. The solid lines are based on the measured rate of metabolism of TPZ (**1**) by HT29 cells and the dashed line on a 5-fold higher rate of drug metabolism. (A) Steady-state concentration gradients as fractions of the plasma concentration (C_p) for O_2 ($C_p = 50$ μM), TPZ, and a TPZ analogue with 6-fold higher diffusion coefficient (as for **14**) assuming $C_p = 40$ μM and the same rate of metabolism for both compounds. (B) Predicted cell killing for the same two compounds. The PD parameters for the faster-diffusing analogue are assumed to be the same as for TPZ.

to kill hypoxic cells in tumors. To address this question, we used a distributed parameter PK/PD model for TPZ to simulate the effect of changing D_{MCL}; the formalism of this model is outlined in the Experimental Section. Briefly, the PK/PD model used the MCL transport parameters to predict PK as a function of distance from blood vessels and used PD parameters (relationship between drug exposure, O_2 concentration, and killing) determined using HT29 single cell suspensions.[18,37] This model follows that reported earlier[15] except that rather than representing the tumor as comprising an oxic and anoxic compartment it models the O_2 gradient from blood vessels and incorporates the O_2 dependence of metabolism and cytotoxicity.[37] Key aspects of this PK/PD model have been validated recently by showing that it correctly predicts the apparent resistance to TPZ of anoxic HT29 cells in MCLs relative to single cells in suspension.[18]

The predictions of the PK/PD model are shown in Figure 5. The steady-state concentration gradient of TPZ is not as steep as for O_2, but the TPZ concentration in the most hypoxic regions is lowered to 62% of that in the perivascular region because of its metabolic consumption during diffusion (Figure 5A). The PK/PD model demonstrates the expected increase in killing with distance (Figure 5B) because of selective activation under hypoxia. When the D_{MCL} is increased 6-fold from 0.4×10^{-6} to 2.4×10^{-6} cm^2 s^{-1} (i.e., to the value for **14**) without changing the rate of TPZ metabolism, the steady-state concentration gradient would be flattened further (analogue in Figure 5A); as a consequence, hypoxic cell killing would be expected to increase, with the surviving fraction of the most hypoxic cells falling from 0.0017 to 2.7×10^{-6} (Figure 5B). Thus, increasing the lipophilicity of TPZ analogues provides a strategy for minimizing the extravascular penetration problem and thereby improving activity against target cells. The gains from increasing D_{MCL} are even greater if the rate of bioreductive metabolism (and hence drug potency) is also increased. Thus, also shown in Figure 5 (as dashed lines) is the effect on exposure and cytotoxicity of increasing the rate of metabolic activation 5-fold. The increased rate of metabolism actually *reduces* hypoxic cell kill in the case of a compound with the same diffusion coefficient as TPZ, due to decreased penetration, but improves hypoxic cell killing by almost 10 logs for the fast-diffusing analogue. We have previously noted that there will be an optimum rate of metabolism for TPZ analogues since a rate that is too rapid impedes penetration and a rate that is too slow limits production of the cytotoxic radical reduction product.[15] The PK/PD model indicates that the optimum rate of metabolism would be shifted to higher values if the diffusion coefficient were increased and that attempts to develop improved analogues by increasing rates of metabolic reduction alone are likely to fail. The rate of metabolism can be modulated by electron-withdrawing or -donating substituents in the A-ring, for example, as noted above with **5**, **6**, **7**, **9**, **10**, and **11**, and this will also have an impact on hypoxia-selective cytotoxic potency.[24,38,39] We conclude that increasing tissue diffusion coefficients by increasing drug lipophilicity has the potential to provide considerably improved TPZ analogues by diminishing the constraint imposed by limited extravascular transport; this would allow development of compounds that are more rapidly activated by enzymatic reduction under hypoxia and would provide much greater activity against hypoxic cells in tumors.

Whether the relationship between log P and D_{MCL} for TPZ analogues can be generalized to other classes of antitumor agents remains to be determined. Initial investigation of analogues with 3-alkyl substituents (replacing the 3-NH_2 group of TPZ) suggests that these may fall on a different line, with higher values of D_{MCL}, possibly because the 3-NH_2 group of TPZ impedes membrane permeation as a consequence of its H-bond donor/acceptor properties. It has been reported for peptide and peptide mimetics that passive membrane permeability is best described by a combination of terms for lipophilicity and hydrogen bond potential.[40,41] However, even if the relationship observed for TPZ analogues is not universal, the present study clearly demonstrates the importance of drug lipophilicity as a determinant of extravascular transport and provides a general methodology for investigating this relationship within congeneric drug series.

Conclusions

The flux of 17 neutral compounds (primarily analogues of the hypoxic cytotoxin tirapazamine) across multicellular layers of HT29 human tumor cells has been determined, and the diffusion coefficients (D_{MCL}) were derived. We demonstrate a marked sigmoidal dependence of D_{MCL} on drug lipophilicity and show that molecular weight is of lesser importance over the size range of typical small molecule drugs. There is some evidence from preliminary data that hydrogen bonds may also affect D_{MCL}. The demonstrated structure−activity relationships provide a strategy for improving the extravascular transport of tirapazamine through the development of more lipophilic analogues. PK/PD modeling shows that the increase in D_{MCL} achievable by raising log P is sufficient to give a large increase in cytotoxicity against hypoxic cells in tumors. This gain is even greater if the kinetics of metabolic activation of

the analogue is increased to take full advantage of the increased rate of diffusion. Assuming that the extravascular transport problem is more severe in tumors than in normal tissue (as expected, given the superior microvascular networks and relative lack of hypoxia in the latter),[42] this is expected to provide analogues with improved therapeutic ratios in vivo.

Inefficient extravascular transport has been identified as one of the key problems in cancer chemotherapy,[43,44] but a lack of experimental models has made it difficult to address this requirement explicitly. The MCL model is potentially a useful tool for determining extravascular transport properties of hits from drug discovery programs and for evaluating this requirement during lead optimization. If the structure−activity relationship demonstrated here for tirapazamine analogues can be generalized to other structural types (and other cell lines), then in silico prediction of extravascular transport properties should be achievable. This would provide a powerful tool for assisting with a critical (and neglected) aspect of lead optimization, although the structural requirements for efficient extravascular transport will need to be expressed within the additional constraints imposed by target interaction (prodrug activation/receptor binding), systemic pharmacokinetics, and toxicology.

Experimental Section

Chemistry. Analyses were carried out in the Microchemical Laboratory, University of Otago, Dunedin, New Zealand. Melting points were determined on an Electrothermal 2300 melting point apparatus. NMR spectra were obtained on a Bruker AM-400 spectrometer at 400 MHz for ^{1}H and 100 MHz for ^{13}C spectra. Spectra were obtained in $CDCl_3$ unless otherwise specified and are referenced to Me_4Si. Chemical shifts and coupling constants were recorded in units of ppm and Hz, respectively. Assignments were determined using COSY, HSQC, and HMBC two-dimensional experiments. Mass spectra were determined on a VG-70SE mass spectrometer using an ionizing potential of 70 eV at a nominal resolution of 1000. High-resolution spectra were obtained at nominal resolutions of 3000, 5000, or 10 000 as appropriate. All spectra were obtained as electron impact (EI) using PFK as the reference unless otherwise stated. Solutions in organic solvents were dried with anhydrous Na_2SO_4, and solvents were evaporated under reduced pressure on a rotary evaporator. Thin-layer chromatography was carried out on aluminum-backed silica gel plates (Merck 60 F_{254}) with visualization of components by UV light (254 nm) or exposure to I_2. Column chromatography was carried out on silica gel (Merck 230−400 mesh). All compounds designated for testing were analyzed at >99% purity by reverse phase HPLC using an Agilent 1100 liquid chromatograph, an Alltima C_{18} (5 μm) stainless steel column (150 mm × 3.2 mm i.d.), and an Agilent 1100 diode array detector. Chromatograms were run using various gradients of aqueous (0.045 M ammonium formate and formic acid at pH 3.5) and organic (80% MeCN/MilliQ water) phases. DCM refers to dichloromethane; ether refers to diethyl ether; DME refers to dimethoxyethane; EtOAc refers to ethyl acetate; EtOH refers to ethanol; MeOH refers to methanol; pet. ether refers to petroleum ether, boiling range 40−60 °C; THF refers to tetrahydrofuran dried over sodium benzophenone ketyl. All solvents were freshly distilled. Compounds were diluted 100-fold from stock solutions (5 mM) in DMSO prior to use.

***N*-Phenyl-1,2,4-benzotriazin-3-amine 1,4-Dioxide (13)**.

***N*-Phenyl-1,2,4-benzotriazin-3-amine 1-Oxide (16)**. Two drops of concentrated HCl were added to a solution of chloride **15**[25] (0.52 g, 2.86 mmol) and aniline (0.78 mL, 8.59 mmol) in DME (10 mL), and the solution was stirred at reflux temperature for 16 h. The solvent was evaporated, and the residue was chromatographed, eluting with 10% EtOAc/pet. ether, to give 1-oxide **16** (334 mg, 49%) as a yellow powder: mp 197−198.5 °C (lit.[26] 199−201 °C); ^{1}H NMR δ 8.32 (d, J = 9.0 Hz, 1 H, H-8), 7.70−7.77 (m, 4 H, H-5, H-6, H-2′, H-6′), 7.37−7.42 (m, 3 H, H-7, H-3′, H-5′), 7.22 (br s, 1 H, NH), 7.13 (dt, J = 7.5, 0.9 Hz, 1 H, H-4′); ^{13}C NMR δ 156.3, 148.1, 138.1, 135.8, 131.6, 129.1 (2), 127.1, 126.1, 123.8, 120.4, 119.7 (2).

***N*-Phenyl-1,2,4-benzotriazin-3-amine 1,4-Dioxide (13)**. A solution of MCPBA (0.99 g, 4.0 mmol) in DCM (10 mL) was added to a stirred solution of 1-oxide **16** (0.64 g, 2.7 mmol) in DCM (100 mL), and the solution was stirred at 20 °C for 2 h. The solvent was evaporated, and the residue was chromatographed, eluting with a gradient (10−20%) of EtOAc/DCM, to give (i) starting material (0.34 g, 50%) spectroscopically identical with the sample prepared above and (ii) 1,4-dioxide **13** (85 mg, 12%) as a red powder: mp 201−203 °C; ^{1}H NMR δ 9.17 (br s, 1 H, NH), 8.37−8.41 (m, 2 H, H-5, H-8), 7.90−7.94 (m, 1 H, H-6), 7.58−7.68 (m, 3 H, H-7, H-3′, H-5′), 7.43 (dd, J = 7.8, 7.4 Hz, 2 H, H-2′, H-6′), 7.21 (t, J = 7.4 Hz, 1 H, H-4′); ^{13}C NMR δ 147.5, 138.0, 136.1, 135.7, 131.3, 129.4 (2), 127.9, 125.2, 121.9, 120.8 (2), 117.8. Anal. ($C_{13}H_{10}N_4O_2$) C, H, N.

***N*-[3-(2-Methoxyethyl)phenyl]-1,2,4-benzotriazin-3-amine 1,4-Dioxide (14)**.

1-(2-Methoxyethyl)-3-nitrobenzene (17). A solution of 3-nitrophenethyl alcohol (1.05 g, 6.3 mmol) in THF (10 mL) was added dropwise to a stirred suspension of NaH (325 mg, 8.1 mmol) in THF (30 mL) at 5 °C, and the mixture was warmed to 20 °C and stirred 30 min. Iodomethane (3.9 mL, 62.5 mmol) was added, and the mixture was stirred at 20 °C for 16 h. The solvent was evaporated and the residue partitioned between EtOAc (100 mL) and water (100 mL). The organic fraction was washed with water (2 × 30 mL) and brine (30 mL) and dried, and the solvent was evaporated. The residue was chromatographed, eluting with 20% EtOAc/pet. ether, to give ether **17** (981 mg, 87%) as a clear oil:[27] ^{1}H NMR δ 8.06−8.11 (m, 2 H, H-2, H-4), 7.57 (d, J = 7.6 Hz, 1 H, H-6), 7.47 (dd, J = 7.9, 7.6 Hz, 1 H, H-5), 3.65 (t, J = 6.5 Hz, 2 H, CH_2O), 3.36 (s, 3 H, OCH_3), 2.98 (t, J = 6.5 Hz, 2 H, CH_2); ^{13}C NMR δ 148.3, 141.3, 135.2, 129.2, 123.7, 121.4, 72.5, 58.8, 35.8.

3-(2-Methoxyethyl)aniline (18). A solution of ether **17** (928 mg, 5.1 mmol) in EtOH (50 mL) with Pd/C (100 mg) was stirred under H_2 (60 psi) for 2 h. The mixture was filtered through Celite and washed with EtOH (2 × 10 mL), and the solvent was evaporated to give aniline **18** (718 mg, 93%) as a pale pink oil: ^{1}H NMR δ 7.08 (dd, J = 7.7, 7.3 Hz, 1 H, H-5), 6.62 (br d, J = 7.3 Hz, 1 H, H-4), 6.51−6.55 (m, 2 H, H-2, H-6), 3.50 (br s, 2 H, NH_2), 3.58 (t, J = 7.2 Hz, 2 H, CH_2O), 3.35 (s, 3 H, OCH_3), 2.80 (t, J = 7.2 Hz, 2 H, CH_2); ^{13}C NMR δ 146.4, 140.1, 129.3, 119.1, 115.7, 113.1, 73.6, 58.6, 36.2; MS (EI$^+$) *m/z* 151 (M^+, 90%), 136 (20), 106 (100); HRMS calcd for $C_9H_{13}NO$ (M^+) *m/z* 151.0997; found, 151.0995.

***N*-[3-(2-Methoxyethyl)phenyl]-1,2,4-benzotriazin-3-amine 1-Oxide (19)**. A solution of chloride **15** (376 mg, 2.1 mmol) and amine **18** (688 mg, 4.6 mmol) in DMSO (20 mL) was heated at 100 °C for 16 h. The solution was partitioned between EtOAc (100 mL) and water (100 mL), the organic fraction was washed with water (2 × 50 mL) and brine (50 mL) and dried, and the solvent was evaporated. The residue was chromatographed, eluting with a gradient (20−50%) of EtOAc/pet. ether, to give 1-oxide **19** (590 mg, 96%) as an orange powder: mp (EtOAc/Et_2O) 122−124 °C; ^{1}H NMR [$(CD_3)_2SO$] δ 10.18 (s, 1 H, NH), 8.22 (dd, J = 8.6, 1.0 Hz, 1 H, H-8), 7.87 (ddd, J = 8.5, 7.1, 1.3 Hz, 1 H, H-6), 7.70−7.76 (m, 3 H, H-5, H-2′, H-6′), 7.47 (ddd, J = 8.6, 7.1, 1.3 Hz, 1 H, H-7), 7.27 (dd, J = 7.9, 7.8 Hz, 1 H, H-5′), 6.94 (d, J = 7.8 Hz, 1 H, H-4′), 3.58 (t, J = 6.8 Hz, 2 H, CH_2O), 3.27 (s, 3 H, OCH_3), 2.82 (t, J = 6.8 Hz, 2 H, CH_2); ^{13}C NMR [$(CD_3)_2SO$] δ 156.3, 147.5, 139.5 (C-1′), 139.1 (C-4a), 135.9 (C-6), 130.9 (C-8a), 128.4 (C-5′), 126.6 (C-5), 125.8 (C-4′), 123.2, 119.8, 119.7, 117.3, 72.6, 57.8, 35.5. Anal. ($C_{16}H_{16}N_4O_2$) C, H, N.

***N*-[3-(2-Methoxyethyl)phenyl]-1,2,4-benzotriazin-3-amine 1,4-Dioxide (14).** H_2O_2 (70%, 260 μL, ca. 5.2 mmol) was added dropwise to a stirred solution of trifluoroacetic

anhydride (730 μL, 5.2 mmol) in DCM (5 mL) at 5 °C. The solution was stirred at 5 °C for 10 min, then warmed to 20 °C and added dropwise to a stirred solution of 1-oxide **19** (307 mg, 1.0 mmol) in $CHCl_3$ (10 mL) at 20 °C. The red solution was stirred for 5 h, diluted with water (10 mL), and extracted with $CHCl_3$ (4 × 10 mL), the combined organic fraction was dried, and the solvent was evaporated. The residue was chromatographed, eluting with a gradient of (0−5%) of MeOH/(50−100%) EtOAc/pet. ether, to give (i) starting material **19** (143 mg, 47%) spectroscopically identical with the sample prepared above and (ii) 1,4-dioxide **14** (62 mg, 19%) as a red solid: mp (EtOAc/Et_2O) 148−149 °C; ^{1}H NMR [$(CD_3)_2SO$] δ 10.11 (s, 1 H, NH), 8.23−8.28 (m, 2 H, H-5, H-8), 8.00 (ddd, J = 8.5, 7.2, 1.0 Hz, 1 H, H-6), 7.65 (ddd, J = 8.6, 7.2, 0.8 Hz, 1 H, H-7), 7.50−7.53 (m, 2 H, H-2′, H-6′), 7.31 (t, J = 8.7, 7.6, 1 H, H-5′), 7.05 (d, J = 7.6 Hz, 1 H, H-4′), 3.57 (t, J = 6.8 Hz, 2 H, CH_2O), 3.26 (s, 3 H, OCH_3), 2.82 (t, J = 6.8 Hz, 2 H, CH_2); ^{13}C NMR [$(CD_3)_2SO$] δ 147.7, 139.6, 138.2, 138.8, 135.5, 131.0, 128.4, 127.7, 124.7, 122.4, 121.1, 118.7, 117.3, 72.5, 57.7, 35.3. Anal. ($C_{16}H_{16}N_4O_3$) C, H, N.

MCL Cultures. MCLs were grown from human HT29 colon carcinoma cells as described elsewhere.[18,29] In brief, 1 × 10^6 cells were seeded on collagen-coated Teflon microporous support membranes (Biopore; average thickness 30 μm) in Millicell-CM cell culture inserts (Millipore Corporation, Bedford, MA) and grown for 3 days submerged in stirred culture medium (αMEM; GIBCO BRL, Grand Island, NY) supplemented with 10% heat-inactivated fetal calf serum (GIBCO BRL, Auckland), penicillin (100 U/mL), streptomycin (100 μg/mL), and 2 mM l-glutamine.

Determination of Diffusion Coefficient in MCLs. Flux through MCLs was measured in a diffusion chamber as described,[23] using MCLs equilibrated for 60 min with 95% O_2/5% CO_2 at 37 °C in the same medium as above. TPZ analogues were added to the "donor" compartment to 50 μM, along with [^{14}C]urea (Amersham Pharmacia Biotech; 40 MBq/mmol, 7.5 kBq/mL), D-[2-^{3}H]mannitol (ICN Pharmaceuticals Inc., Irvine, CA; 40 MBq/mmol, 20 kBq/mL), and 9(10*H*)-acridone (Sigma-Aldrich, Castle Hill, NSW; 10 μM). Samples were taken from both the donor and receiver compartment for up to 5 h. An aliquot was assayed for radioactivity by dual-label liquid scintillation counting in a Packard Tri-Carb 1500 liquid scintillation analyzer (Packard Instrument Company, Meriden, CT) using Emulsifier-Safe water-accepting scintillant (Packard), and the balance was frozen for subsequent HPLC analysis. The concentration−time profiles of [^{14}C]urea in the donor and receiver compartments were numerically fitted to Fick's second law to estimate the average thickness of each MCL (ca. 175 μm), using the measured value of D_{MCL} for [^{14}C]-urea in HT29 MCLs (0.45 × 10^{-6} cm^2 s^{-1}).[18] The effective diffusion coefficient of each compound was also determined in the collagen-coated Teflon porous support membrane (D_s) without an MCL present. This latter parameter also takes into account the effect of the unstirred boundary layers on each side of the membrane or MCL. D_{MCL} was then determined by fitting the concentration−time profile in both the donor and receiver simultaneously to a Fickian diffusion model with the support membrane and MCL in series as described previously,[23] with addition of reaction terms in the MCL when necessary.

HPLC. Samples (200 μL) were deproteinized by addition of 4 μL of 70% (v/v) perchloric acid and chilling on ice followed by centrifugation (12000×*g* for 5 min at 4 °C) and subsequent neutralization of the supernatant with 50% (v/v) ammonia (31.5 μL/mL supernatant). Concentrations of the TPZ analogues were determined by reverse phase HPLC (Alltima C_8 5 μm column, 150 mm × 2.1 mm; Alltech Associated Inc., Deerfield, IL) using an Agilent HP1100 equipped with a diode-array detector. Mobile phases were gradients of 80% acetonitrile/20% H_2O (v/v) in 450 mM ammonium formate, pH 4.5, at 0.3 mL/min. Quantitation was based on calibration curves in mobile phase (0.1−100 μM), corrected for recovery from medium with serum determined by assaying known concentrations (0.1−100 μM) for each compound under the same conditions.

Partition Coefficients. The octanol−water partition coefficient (P) was measured using the shake-flask method,[28] using GPR-grade octanol (BDH Laboratory Supplies). Briefly, lipophilic drugs were dissolved directly in octanol-saturated PBS (137 mM NaCl, 2.68 mM KCl, 1.47 mM KH_2PO_4, 8.10 mM Na_2HPO_4, pH 7.4), and hydrophilic drugs were dissolved in PBS-saturated octanol to 25−100 μM. Equal volumes of PBS and octanol were mixed on a Bellco roller drum (Bellco Glass, Inc., NJ) at 20 rpm for 3 h at ambient temperature. The two solvent layers were separated after a brief spin and analyzed by HPLC directly (aqueous layer) or after addition of 4 volumes of methanol (organic layer).

Mathematical Modeling. Using the transport parameters governing extravascular diffusion derived from MCL flux studies and the plasma PK, we calculated the concentration−time profile for TPZ and analogues as a function of position, x, and time, t, in the extravascular compartment as previously described.[37] First, the oxygen diffusion gradient (which determines the rate of hypoxic drug metabolism) was calculated in the same way as for TPZ (below) using representative literature values (diffusion coefficient 1.25 × 10^{-5} cm^2 s^{-1},[45] consumption rate 0.022 cm^3 g^{-1} min^{-1},[46] input capillary concentration of 50 μM [ca. 40 mmHg] O_2[47]). A planar geometry (i.e., bidirectional diffusion into a slab of tissue) was assumed as a compromise between radial outward diffusion in a Krogh cylinder and radial inward diffusion for a tumor cord surrounded by stroma. Under these conditions the O_2 concentration falls to 10 ppm at 95 μm from the plasma compartment. It was also assumed that a small population of cells survives transiently under this very low oxygen tension, up to 5 μm beyond the diffusion limit of O_2. This simulation gives a radiobiologically hypoxic fraction (proportion of cells at <4 μM O_2) of 36%.

The recently determined kinetics of the metabolic activation of TPZ[18] and its oxygen dependence[37] were used to simulate TPZ metabolism in tissue as follows:

$$\frac{\partial M}{\partial t} = \left(\frac{K}{[O_2] + K}\right)\left(k_{met}[TPZ] + \frac{V_{max}[TPZ]}{K_m + [TPZ]}\right) \qquad (2)$$

where $M(x,t)$ is the cumulative amount of TPZ metabolized per unit intracellular volume, K is the oxygen concentration required to halve the rate of TPZ metabolism (1.21 μM),[37] and k_{met} (0.78 min^{-1}), V_{max} (8.5 μM min^{-1}), and K_m (3.5 μM) are the first-order and Michaelis−Menten parameters governing TPZ metabolism in anoxic HT29 cells.[18] The following reaction−diffusion equation

$$\frac{\partial[TPZ]}{\partial t} = D\frac{\partial^2[TPZ]}{\partial x^2} - \phi\frac{\partial M}{\partial t} \qquad (3)$$

was then solved for [TPZ] at a distance x and time t using the appropriate tissue diffusion coefficient (D), which is assumed to be identical to the experimentally determined D_{MCL} and intracellular volume fraction (ϕ). The boundary conditions were defined by the plasma PK profile in humans in recent clinical trials[48−50] where TPZ is infused over 2 h at a dose of 390 mg/m^2, as calculated using PK parameters from the phase I studies.[51,52] This would produce a maximum area under the plasma concentration time curve (AUC_p) of 150 μM h with a plasma concentration of 40 μM over the first 2.5 h followed by a first-order decay with a half-life of 47 min. This simulation provided the drug PK profile as a function of distance within the extravascular compartment, which rapidly reaches the steady state profile shown in Figure 5A for the first 2.5 h and then decays with a similar half-life to that of drug in plasma. This was used in conjunction with a recently determined PD model for TPZ cytotoxicity[18] to calculate cell killing as a function of distance. Briefly, the PD model assumes that the log cell kill under steady-state conditions is proportional to

the product of the TPZ concentration and the cumulative metabolism of TPZ to its active radical:

$$-\log(\mathrm{SF}) = \gamma \times [\mathrm{TPZ}] \times M \quad (4)$$

where SF is the surviving fraction and γ is the value ($2.33 \times 10^{-5}\ \mu\mathrm{M}^{-2}$) determined for HT29 cells.[18] The cell kill predicted by this model for the two compounds is shown in Figure 5B.

Acknowledgment. The authors thank Dr. Maruta Boyd, Sisira Kumara, and Li Fong Leong for technical support. This work was supported by Grant No. CA82566 from the U.S. National Cancer Institute (F.B.P., J.R.S., H.D.S.L., K.O.H., M.P.H.), the Health Research Council of New Zealand (W.R.W.), and the Auckland Division of the Cancer Society of New Zealand (W.A.D.).

Supporting Information Available: Elemental analysis data for compounds **13**, **14**, **18**, and **19**. This material is available free of charge via the Internet at http://pubs.acs.org.

References

(1) Fujimori, K.; Covell, D. G.; Fletcher, J. E.; Weinstein, J. N. Modeling analysis of the global and microscopic distribution of immunoglobulin G, F(ab′)$_2$, and Fab in tumors. *Cancer Res.* **1989**, *49*, 5656−5663.
(2) van Osdol, W.; Fujimori, K.; Weinstein, J. N. An analysis of monoclonal antibody distribution in microscopic tumor nodules: consequences of a "binding site barrier". *Cancer Res.* **1991**, *51*, 4776−4784.
(3) Rowe-Jones, D. C. The penetration of cytotoxins into malignant tumours. *Br. J. Cancer* **1968**, *22*, 155−162.
(4) Jain, R. K.; Weissbrod, J. M.; Wei, J. Mass transport in tumors: characterization and applications to chemotherapy. *Adv. Cancer Res.* **1980**, *33*, 251−310.
(5) Blasberg, R.; Horowitz, M.; Strong, J.; Molnar, P.; Patlak, C.; Owens, E.; Fenstermacher, J. Regional measurements of [^{14}C]-misonidazole distribution and blood flow in subcutaneous RT-9 experimental tumors. *Cancer Res.* **1985**, *45*, 1692−1701.
(6) Kerr, D. J.; Kaye, S. B. Aspects of cytotoxic drug penetration with particular reference to anthracyclines. *Cancer Chemother. Pharmacol.* **1987**, *19*, 1−5.
(7) Simpson-Herren, L.; Noker, P. E. Diversity of penetration of anticancer agents into solid tumours. *Cell Proliferation* **1991**, *24*, 355−365.
(8) Jain, R. K. The next frontier of molecular medicine: delivery of therapeutics. *Nat. Med.* **1998**, *4*, 655−657.
(9) Tannock, I. F. Conventional cancer therapy: promise broken or promise delayed? *Lancet* **1998**, *351* (Suppl. 2), 9−16.
(10) Brown, J. M. SR 4233 (tirapazamine): a new anticancer drug exploiting hypoxia in solid tumours. *Br. J. Cancer* **1993**, *67*, 1163−1170.
(11) Denny, W. A.; Wilson, W. R. Tirapazamine: a bioreductive anticancer drug that exploits tumour hypoxia. *Expert Opin. Invest. Drugs* **2000**, *9*, 2889−2901.
(12) Baker, M. A.; Zeman, E. M.; Hirst, V. K.; Brown, J. M. Metabolism of SR 4233 by Chinese hamster ovary cells: basis of selective hypoxic cytotoxicity. *Cancer Res.* **1988**, *48*, 5947−5952.
(13) Siim, B. G.; van Zijl, P. L.; Brown, J. M. Tirapazamine-induced DNA damage measured using the comet assay correlates with cytotoxicity towards hypoxic tumour cells in vitro. *Br. J. Cancer* **1996**, *73*, 952−960.
(14) Durand, R. E.; Olive, P. L. Evaluation of bioreductive drugs in multicell spheroids. *Int. J. Radiat. Oncol., Biol., Phys.* **1992**, *22*, 689−692.
(15) Hicks, K. O.; Fleming, Y.; Siim, B. G.; Koch, C. J.; Wilson, W. R. Extravascular diffusion of tirapazamine: effect of metabolic consumption assessed using the multicellular layer model. *Int. J. Radiat. Oncol., Biol., Phys.* **1998**, *42*, 641−649.
(16) Kyle, A. H.; Minchinton, A. I. Measurement of delivery and metabolism of tirapazamine to tumour tissue using the multilayered cell culture model. *Cancer Chemother. Pharmacol.* **1999**, *43*, 213−220.
(17) Baguley, B. C.; Hicks, K. O.; Wilson, W. R. Tumour cell cultures in drug development. In *Anticancer Drug Development*; Baguley, B. C., Kerr, D. J., Eds.; Academic Press: San Diego, CA, 2002; pp 269−284.
(18) Hicks, K. O.; Pruijn, F. B.; Sturman, J. R.; Denny, W. A.; Wilson, W. R. Multicellular resistance to tirapazamine is due to restricted extravascular transport: a pharmacokinetic/pharmacodynamic study in HT29 multicellular layer cultures. *Cancer Res.* **2003**, *63*, 5970−5977.
(19) Kubinyi, H. Lipophilicity and biological activity. *Arzneim.-Forsch.* **1979**, *29*, 1067−1080.
(20) Lieb, W. R.; Stein, W. D. Simple diffusion across the membrane bilayer. In *Transport and Diffusion across Cell Membranes*; Stein, W. D., Ed.; Academic Press: Orlando,FL, 1986; pp 69−112.
(21) Cowan, D. S.; Hicks, K. O.; Wilson, W. R. Multicellular membranes as an in vitro model for extravascular diffusion in tumours. *Br. J. Cancer, Suppl.* **1996**, *27*, S28−S31.
(22) Minchinton, A. I.; Wendt, K. R.; Clow, K. A.; Fryer, K. H. Multilayers of cells growing on a permeable support. An in vitro tumour model. *Acta Oncol.* **1997**, *36*, 13−16.
(23) Hicks, K. O.; Pruijn, F. B.; Baguley, B. C.; Wilson, W. R. Extravascular transport of the DNA intercalator and topoisomerase poison *N*-[2-(dimethylamino)ethyl]acridine-4-carboxamide (DACA): diffusion and metabolism in multicellular layers of tumor cells. *J. Pharmacol. Exp. Ther.* **2001**, *297*, 1088−1098.
(24) Hay, M. P.; Gamage, S. A.; Kovacs, M. S.; Pruijn, F. B.; Anderson, R. F.; Patterson, A. V.; Wilson, W. R.; Brown, J. M.; Denny, W. A. Structure−activity relationships of 1,2,4-benzotriazine 1,4-dioxides as hypoxia-selective analogues of tirapazamine. *J. Med. Chem.* **2003**, *46*, 169−182.
(25) Robbins, R. F.; Schofield, K. Polyazabicyclic compounds. Part II. Further derivatives of benzo-1,2,4-triazine. *J. Chem. Soc.* **1957**, 3186−3194.
(26) Pazdera, P.; Potacek, M. *N*-Ethyl substituted 2-nitrophenylguanidines. II Cyclization. *Chem. Pap.* **1989**, *43*, 107−112.
(27) Norman, R. O. C.; Radda, G. K. The ortho:para ratio in aromatic substitution. Part 1. The nitration of methyl phenethyl ether. *J. Chem. Soc.* **1961**, 3030−3037.
(28) Siim, B. G.; Hicks, K. O.; Pullen, S. M.; van Zijl, P. L.; Denny, W. A.; Wilson, W. R. Comparison of aromatic and tertiary amine *N*-oxides of acridine DNA intercalators as bioreductive drugs. Cytotoxicity, DNA binding, cellular uptake, and metabolism. *Biochem. Pharmacol.* **2000**, *60*, 969−978.
(29) Wilson, W. R.; Pullen, S. M.; Hogg, A.; Hobbs, S. M.; Pruijn, F. B.; Hicks, K. O. In vitro and in vivo models for evaluation of GDEPT: quantifying bystander killing in cell cultures and tumors. In *Suicide Gene Therapy: Methods and Reviews*; Springer, C. J., Ed.; Humana Press: Totowa, NJ, 2003; pp 403−432.
(30) Cussler, E. L. Values of diffusion coefficients. In *Diffusion, Mass Transfer in Fluid Systems*, 2nd ed.; Cussler, E. L., Ed.; Cambridge University Press: Cambridge and New York, 1997; pp 101−141.
(31) Cummings, J.; Boyd, G.; Macpherson, J. S.; Wolf, H.; Smith, G.; Smyth, J. F.; Jodrell, D. I. Factors influencing the cellular accumulation of SN-38 and camptothecin. *Cancer Chemother. Pharmacol.* **2002**, *49*, 194−200.
(32) Schmittmann, G.; Rohr, U. D. Comparison of the permeability surface product (*PS*) of the blood capillary wall in skeletal muscle tissue of various species and in vitro porous membranes using hydrophilic drugs. *J. Pharm. Sci.* **2000**, *89*, 115−127.
(33) Artursson, P. Epithelial transport of drugs in cell culture. I: A model for studying the passive diffusion of drugs over intestinal absorptive (Caco-2) cells. *J. Pharm. Sci.* **1990**, *79*, 476−482.
(34) Adson, A.; Burton, P. S.; Raub, T. J.; Barsuhn, C. L.; Audus, K. L.; Ho, N. F. Passive diffusion of weak organic electrolytes across Caco-2 cell monolayers: uncoupling the contributions of hydrodynamic, transcellular, and paracellular barriers. *J. Pharm. Sci.* **1995**, *84*, 1197−1204.
(35) Dearden, J. C. Molecular structure and drug transport. In *Comprehensive Medicinal Chemistry: The Rational Design, Mechanistic Study & Therapeutic Application of Chemical Compounds*, 1st ed.; Hansch, C., Sammes, P. G., Taylor, J. B., Eds.; Pergamon Press: Oxford and New York, 1990; pp 375−411.
(36) Mastro, A. M.; Babich, M. A.; Taylor, W. D.; Keith, A. D. Diffusion of a small molecule in the cytoplasm of mammalian cells. *Proc. Natl. Acad. Sci. U.S.A.* **1984**, *81*, 3414−3418.
(37) Hicks, K. O.; Siim, B. G.; Pruijn, F. B.; Wilson, W. R. Oxygen dependence of the metabolic activation and cytotoxicity of tirapazamine: implications for extravascular transport and activity in tumors. *Radiat. Res.* **2004**, *161*, 656−666.
(38) Zeman, E. M.; Baker, M. A.; Lemmon, M. J.; Pearson, C. I.; Adams, J. A.; Brown, J. M.; Lee, W. W.; Tracy, M. Structure−activity relationships for benzotriazine di-*N*-oxides. *Int. J. Radiat. Oncol., Biol., Phys.* **1989**, *16*, 977−981.
(39) Kelson, A. B.; McNamara, J. P.; Pandey, A.; Ryan, K. J.; Dorie, M. J.; McAfee, P. A.; Menke, D. R.; Brown, J. M.; Tracy, M. 1,2,4-Benzotriazine 1,4-dioxides. An important class of hypoxic cytotoxins with antitumor activity. *Anti-Cancer Drug Des.* **1998**, *13*, 575−592.
(40) Goodwin, J. T.; Conradi, R. A.; Ho, N. F.; Burton, P. S. Physicochemical determinants of passive membrane permeability: role of solute hydrogen-bonding potential and volume. *J. Med. Chem.* **2001**, *44*, 3721−3729.

(41) Stenberg, P.; Luthman, K.; Artursson, P. Prediction of membrane permeability to peptides from calculated dynamic molecular surface properties. *Pharm. Res.* **1999**, *16*, 205−212.
(42) Brown, J. M.; Giaccia, A. J. The unique physiology of solid tumors: opportunities (and problems) for cancer therapy. *Cancer Res.* **1998**, *58*, 1408−1416.
(43) Lankelma, J. Tissue transport of anti-cancer drugs. *Curr. Pharm. Des.* **2002**, *8*, 1987−1993.
(44) Tannock, I. F. Tumor physiology and drug resistance. *Cancer Metastasis Rev.* **2001**, *20*, 123−132.
(45) Grote, J.; Süsskind, R.; Vaupel, P. Oxygen diffusivity in tumor tissue (DS-carcinosarcoma) under temperature conditions within the range of 20−40 °C. *Pfluegers Arch.* **1977**, *372*, 37−42.
(46) Dewhirst, M. W.; Secomb, T. W.; Ong, E. T.; Hsu, R.; Gross, J. F. Determination of local oxygen consumption rates in tumors. *Cancer Res.* **1994**, *54*, 3333−3336.
(47) Dewhirst, M. W.; Ong, E. T.; Klitzman, B.; Secomb, T. W.; Vinuya, R. Z.; Dodge, R.; Brizel, D.; Gross, J. F. Perivascular oxygen tensions in a transplantable mammary tumor growing in a dorsal flap window chamber. *Radiat. Res.* **1992**, *130*, 171−182.
(48) Hoff, P. M.; Saad, E. D.; Ravandi-Kashani, F.; Czerny, E.; Pazdur, R. Phase I trial of i.v. administered tirapazamine plus cyclophosphamide. *Anti-Cancer Drugs* **2001**, *12*, 499−503.
(49) von Pawel, J.; von Roemeling, R.; Gatzemeier, U.; Boyer, M.; Elisson, L. O.; Clark, P.; Talbot, D.; Rey, A.; Butler, T. W.; Hirsh, V.; Olver, I.; Bergman, B.; Ayoub, J.; Richardson, G.; Dunlop, D.; Arcenas, A.; Vescio, R.; Viallet, J.; Treat, J. Tirapazamine plus cisplatin versus cisplatin in advanced non-small-cell lung cancer: A report of the international CATAPULT I study group. Cisplatin and tirapazamine in subjects with advanced previously untreated non-small-cell lung tumors. *J. Clin. Oncol.* **2000**, *18*, 1351−1359.
(50) Bedikian, A. Y.; Legha, S. S.; Eton, O.; Buzaid, A. C.; Papadopoulos, N.; Plager, C.; McIntyre, S.; Viallet, J. Phase II trial of escalated dose of tirapazamine combined with cisplatin in advanced malignant melanoma. *Anti-Cancer Drugs* **1999**, *10*, 735−739.
(51) Graham, M. A.; Senan, S.; Robin, H., Jr.; Eckhardt, N.; Lendrem, D.; Hincks, J.; Greenslade, D.; Rampling, R.; Kaye, S. B.; von Roemeling, R.; Workman, P. Pharmacokinetics of the hypoxic cell cytotoxic agent tirapazamine and its major bioreductive metabolites in mice and humans: retrospective analysis of a pharmacokinetically guided dose-escalation strategy in a phase I trial. *Cancer Chemother. Pharmacol.* **1997**, *40*, 1−10.
(52) Johnson, C. A.; Kilpatrick, D.; von Roemeling, R.; Langer, C.; Graham, M. A.; Greenslade, D.; Kennedy, G.; Keenan, E.; O'Dwyer, P. J. Phase I trial of tirapazamine in combination with cisplatin in a single dose every 3 weeks in patients with solid tumors. *J. Clin. Oncol.* **1997**, *15*, 773−780.

JM049549P